# A common signaling cascade may underlie "addiction" to the Src, BCR-ABL, and EGF receptor oncogenes

Sreenath V. Sharma,[1] Patrycja Gajowniczek,[1] Inna P. Way,[1] Diana Y. Lee,[1] Jane Jiang,[2] Yuki Yuza,[2] Marie Classon,[1] Daniel A. Haber,[1] and Jeffrey Settleman[1,*]

[1] Massachusetts General Hospital Cancer Center and Harvard Medical School, 149 13th Street, Charlestown, Massachusetts 02129
[2] Dana-Farber Cancer Research Institute, 44 Binney Street, Boston, Massachusetts 02115
*Correspondence: settleman@helix.mgh.harvard.edu

## Summary

**"Oncogene addiction" describes an unexplained dependency of cancer cells on a particular cellular pathway for survival or proliferation. We report that differential attenuation rates of prosurvival and proapoptotic signals in oncogene-dependent cells contribute to cell death following oncogene inactivation. Src-, BCR-ABL-, and EGF receptor-dependent cells exhibit a similar profile of signal attenuation following oncogene inactivation characterized by rapid diminution of phospho-ERK, -Akt, and -STAT3/5, and a delayed accumulation of the proapoptotic effector phospho-p38 MAPK. These findings implicate a transient imbalance in survival and apoptotic oncogenic outputs in the apoptotic response to oncogene inactivation. Moreover, these observations implicate a common profile of signal attenuation for multiple oncogenes and suggest that "addiction" associated with apoptosis reflects an active rather than a passive process.**

## Introduction

"Oncogene addiction" is a term that was first coined by Bernard Weinstein to describe the apparent acquisition of dependency by tumor cells on a single oncogenic activity (Weinstein, 2000, 2002; Weinstein et al., 1997). This phenomenon has been most clearly illustrated in several different transgenic mouse models of tumorigenesis and is characterized by the proliferative arrest, differentiation, and/or apoptosis of tumor cells upon the acute inactivation of an oncogene that initially contributed to the tumor phenotype. For example, in a leukemic model in which inducible transgenic Myc overexpression causes T cell and myeloid leukemias, switching off the Myc oncogene causes tumor cells to undergo growth arrest, differentiation, and apoptotic cell death (Felsher and Bishop, 1999). Similarly, in a transgenic model of BCR-ABL-induced leukemia, switching off the transgene results in rapid apoptosis of leukemic cells (Huettner et al., 2000). The oncogene addiction phenomenon appears to apply to solid tumors as well, since in a model of conditional transgenic H-Ras-induced mouse melanomas, turning off the activated Ras gene causes massive apoptosis within tumors (Chin et al., 1999).

In addition to these transgenic oncogene models, cell culture studies of human cancer cells have further substantiated the concept that tumor cells can become dependent on a single oncogenic pathway for their sustained proliferation or survival. For example, human pancreatic cancer cell lines harboring a mutationally activated K-Ras oncogene can be growth inhibited by introducing antisense K-Ras oligonucleotides (Aoki et al., 1997). Similarly, selective kinase inhibitors such as imatinib (Gleevec), which targets the BCR-ABL fusion kinase (Druker et al., 1996; Gambacorti-Passerini et al., 1997), or gefitinib (Iressa) or erlotinib (Tarceva), which target the EGF receptor kinase (Mukohara et al., 2005), can efficiently kill a subset of cultured tumor cells that express those oncogenes. Such findings seem to indicate that many tumor cells, despite the accumulation of multiple genetic alterations, retain dependency on a limited number of oncogenes that initially drove them to a malignant phenotype.

The apparent dependency on individual oncogenes exhibited by tumor cells potentially reveals an "Achilles' heel," or vulnerable point, within such cells that renders them susceptible to the activities of antitumor agents that selectively target these oncogene products (Weinstein, 2002). Indeed, examples of dramatic clinical response have been observed in a subset of BCR-ABL-positive chronic myelogenous leukemia patients treated with imatinib (O'Dwyer et al., 2003). Similarly, a subset of patients with non-small cell lung cancer, where mutationally

### SIGNIFICANCE

**The phenomenon of "oncogene addiction" has now been well documented in multiple mouse tumor models and cancer cell lines. Moreover, oncogene addiction may account for the dramatic clinical responses reported in some cancer patients treated with targeted kinase inhibitors. However, a molecular mechanism to explain oncogene addiction has been elusive. Our findings suggest that differential decay rates of prosurvival and proapoptotic signals emanating from an oncoprotein, such as an activated kinase, can contribute to tumor cell death following acute inactivation of an oncogene upon which they have become dependent. Our findings attempt to provide a molecular mechanism for oncogene dependency, and they may have important implications for the therapeutic use of targeted kinase inhibitors.**

activated or amplified EGF receptors are sometimes observed, exhibit striking clinical responses to gefitinib and erlotinib (Lynch et al., 2004; Paez et al., 2004; Pao et al., 2004). It is believed that such responses similarly reflect the phenomenon of oncogene addiction, thereby highlighting its importance in the context of cancer therapeutics that target activated oncoproteins.

Despite accumulating evidence (largely derived from transgenic mouse models, cell culture studies of human cancer cell lines, and clinical studies of targeted kinase inhibitors) that oncogene addiction is a widespread and important phenomenon, a molecular mechanism to explain it has yet to be clearly elucidated. It has been suggested that the ''circuitry'' of a cancer cell has somehow been corrupted such that it acquires a dependency on signaling pathways that are not normally required in the cell from which the tumor cell was derived (Weinstein, 2002). This could certainly be true, although it has been difficult to prove this experimentally. We have recently proposed a related but distinct hypothesis to explain oncogene addiction (Sharma et al., 2006). We propose that differential attenuation rates among the multiple proapoptotic and prosurvival signals emanating from an activated oncogene result in a transient imbalance in signaling. This imbalance results from the fact that survival signals are relatively short-lived following acute inactivation of the oncogene, while proapoptotic signals persist sufficiently long to produce an apoptotic outcome. To test this theoretical model experimentally, we have examined the attenuation kinetics of known survival effectors following the inactivation of the Src, BCR-ABL, and EGF receptor oncogenes in several cell culture models associated with oncogene dependency. We determined that a common profile of signal attenuation involving the ERK, Akt, and STAT3/5 proteins is associated with oncogene inactivation in each of these cases, and that in each setting, a temporally delayed accumulation of at least one proapoptotic effector, phospho-p38 MAP kinase, is observed. Based on these and additional findings described below, we conclude that a shared mechanism of differential signal attenuation can contribute to the oncogene addiction phenomenon in multiple different contexts.

## Results

### Modeling oncogene addiction in cells dependent on the BCR-ABL oncogene

To model the phenomenon of oncogene addiction in cultured cells, we took advantage of a previously described cell line, TonB210.1, in which the BCR-ABL oncoprotein that is detected in the vast majority of human chronic myelogenous leukemias (CML), is expressed in a doxycycline-regulated manner (Klucher et al., 1998). TonB210.1 cells were derived from an interleukin-3 (IL-3)-dependent hematopoietic cell line (BAF3), and expression of the BCR-ABL protein in these cells renders them IL-3 independent in a cell viability assay. As previously reported (Klucher et al., 1998), these cells undergo massive apoptotic cell death within 48–72 hr following disruption of BCR-ABL expression (data not shown). This dependency on maintained BCR-ABL survival signaling appears to model the well-established clinical response to ABL kinase inhibitors seen in some CML patients.

We observed that levels of BCR-ABL protein in TonB210.1 cells begin to decline within 8 hr of doxycycline treatment (Figure 1), and this is accompanied by a concomitant decrease in the phosphorylation of several major phospho-tyrosine-containing proteins (including BCR-ABL itself), as revealed by immunoblotting of cell lysates with a phospho-tyrosine antibody (Figure 1). In these doxycycline-treated cells, morphologic indications of apoptosis become apparent within 8 hr of treatment, and cleaved PARP, a marker of apoptosis, can also be detected at this time point (data not shown). Between 24 and 48 hr following treatment, massive apoptosis becomes evident, and the vast majority of cells are dead within 72 hr. Thus, as previously described, these cells are highly dependent on BCR-ABL expression for their survival.

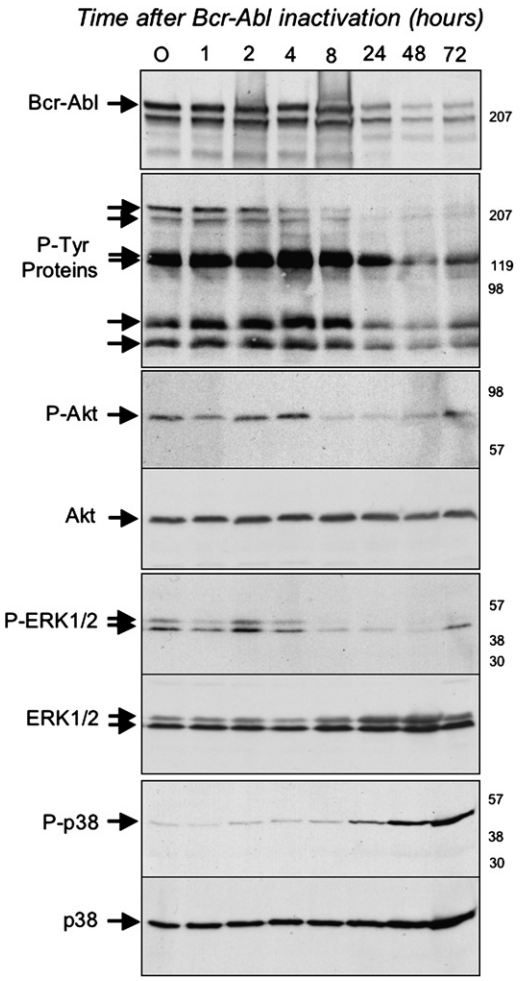


**Figure 1.** Modulation of signaling following acute Bcr-Abl inactivation in TonB210.1 cells

Bcr-Abl was induced in TonB210.1 cells by doxycycline treatment for 18 hr. Bcr-Abl was then inactivated by the removal of doxycycline, and at various times postinactivation Bcr-Abl cells were harvested and their proteins were analyzed by SDS-PAGE followed by western blotting using antibodies directed against Bcr, phospho-tyrosine, phospho-Akt (P-Akt), Akt, phospho-ERK1/2 (P-ERK1/2), ERK1/2, phospho-p38 (P-p38), and p38. Times postinactivation of Bcr-Abl (in hours) are indicated at the top of each lane, the relative migrations of the relevant proteins are indicated on the left-hand side of each autoradiogram, and to the right of each autoradiogram are indicated the relative migrations of molecular weight standards. In the second panel, arrows point to several unidentified proteins whose tyrosine phosphorylation appears to decrease upon Bcr-Abl inactivation.

To determine the kinetics of signal attenuation associated with known downstream mediators of cell survival in this setting, we examined the phosphorylation status of Akt, STAT5, and

ERK1/2 (Steelman et al., 2004). As shown in Figure 1 (and data not shown), each of these proteins is phosphorylated for as long as BCR-ABL protein is active (up to 4 hr). At 8 hr post-doxycycline treatment, concomitant with BCR-ABL inactivation, the phosphorylation of each of the proteins is substantially diminished (Figure 1 and data not shown). Thus, these three "survival effectors" are each rapidly inactivated following disruption of BCR-ABL activity. We also examined the phosphorylation status of the p38 MAP kinase, an established downstream target of BCR-ABL that has been implicated in proapoptotic signaling in some contexts (Bandyopadhyay et al., 2004). Interestingly, while phospho-p38 MAP kinase levels are barely detectable prior to BCR-ABL inactivation, a clear increase in phospho-p38 is observed within 24 hr of doxycycline treatment, suggesting that a temporally delayed activation of p38 contributes to the apoptotic response that follows acute inactivation of BCR-ABL (Figure 1).

### Modeling oncogene addiction in cells dependent on a mutationally activated EGF receptor

We next wanted to determine whether the inactivation of survival effectors and subsequent accumulation of activated p38 that was observed upon BCR-ABL inactivation could extend to other cell culture models of oncogene dependency. Therefore, we took advantage of another BAF3-derived cell line in which expression of a mutationally activated form of the EGF receptor that has been detected in a subset of non-small cell lung cancers confers IL-3-independent cell survival (Jiang et al., 2005). In these cells, treatment with the selective EGF receptor kinase inhibitor gefitinib results in the virtual complete inactivation of EGFR autophosphorylating activity within 4 hr, and massive apoptotic cell death within 72 hr, as previously reported (Jiang et al., 2005) (Figure 2 and data not shown). As was seen in the TonB210.1 cells upon inactivation of BCR-ABL, cleaved PARP can be detected in these cells within 24 hr of EGFR inactivation (Figure 2). Moreover, within 4 hr of gefitinib treatment, levels of phospho-STAT5, -ERK1/2, and -Akt are all substantially reduced (Figure 2), and between 8 and 24 hr, phospho-p38 levels accumulate (Figure 2). Thus, models of oncogene dependency driven by either BCR-ABL or EGFR appear to involve a shared mechanism of signal attenuation following oncogene inactivation that involves the relatively rapid decay of survival signaling followed by a delayed activation of the p38 proapoptotic kinase.

### Modeling Src kinase dependency using a temperature-sensitive switch

Like BCR-ABL and EGFR kinases, the Src kinase has also been implicated in human tumorigenesis and can also transduce pro-survival as well as proapoptotic activities. This signaling duality of Src has been most clearly demonstrated using a fibroblast cell line in which a temperature-sensitive activated c-Src mutant (Maroney et al., 1992) is expressed to produce a malignant phenotype associated with morphologic transformation (Johnson et al., 2000). When cultured in 10% serum at 39.5°C, the nonpermissive temperature (Src is inactive), these cells exhibit a relatively flat, nontransformed appearance in culture. When the temperature is shifted to 35°C, the permissive temperature, these cells rapidly become spindle shaped and refractile, exhibiting clear characteristics of Src-transformed fibroblasts (Figures 3A and 3B). When these cells are shifted to 39.5°C, and the serum concentration is reduced to 0.2%, substantial levels of apoptosis are observed within 2 hr of the temperature shift (Figures 3C and 3D). Significantly, the parental fibroblasts from which these Src-transformed cells were derived do not undergo apoptosis in reduced serum, even when shifted to 39.5°C (data not shown). Thus, this cell culture model appears to represent an additional setting in which an oncogene addiction-like phenomenon is involved.

By examining phospho-proteins in these cells following acute Src inactivation, we determined that, within 30 min of Src

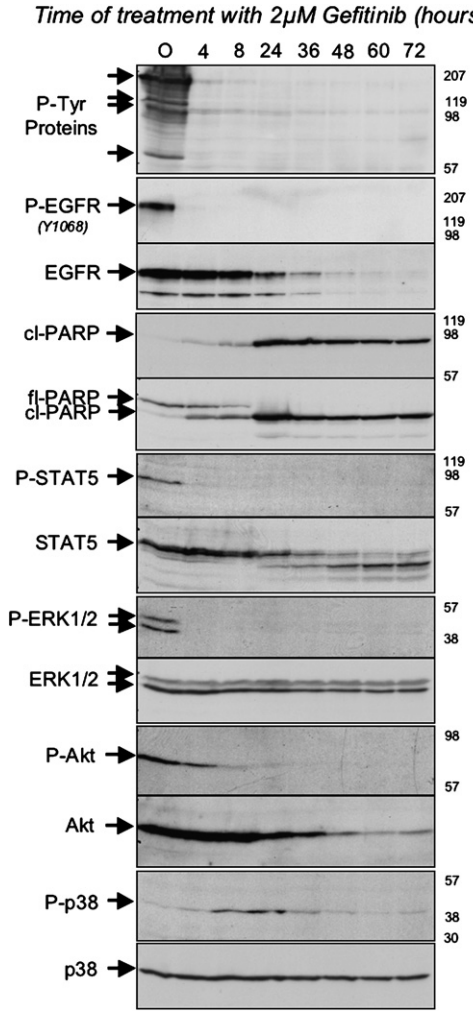


**Figure 2.** Modulation of signaling following acute EGFR(L858R) inactivation in BaF3-EGFR(L858R) cells

BaF3-EGFR(L858R) cells constitutively express the L858R-activating mutation in EGFR, which renders the BaF3 cells independent of IL-3. EGFR(L858R) was inactivated by treating cells with 2 μM of gefitinib, and at various times posttreatment cells were harvested and their proteins were analyzed by SDS-PAGE followed by western blotting using antibodies directed against phospho-tyrosine (P-Tyr proteins), phospho-EGFR$^{Y1068}$ (P-EGFR), EGFR, cleaved PARP (cl-PARP), full-length PARP (fl-PARP), phospho-STAT5 (P-STAT5), STAT5, phospho-ERK1/2 (P-ERK1/2), ERK1/2, phospho-Akt (P-Akt), Akt, phospho-p38 (P-p38), and p38. Times posttreatment with gefitinib (in hours) are indicated at the top of each lane, the relative migrations of the relevant proteins are indicated on the left-hand side of each autoradiogram, and to the right of each autoradiogram are indicated the relative migrations of molecular weight standards. In the top panel, arrows point to several unidentified proteins whose tyrosine phosphorylation appears to decrease upon v-src inactivation.

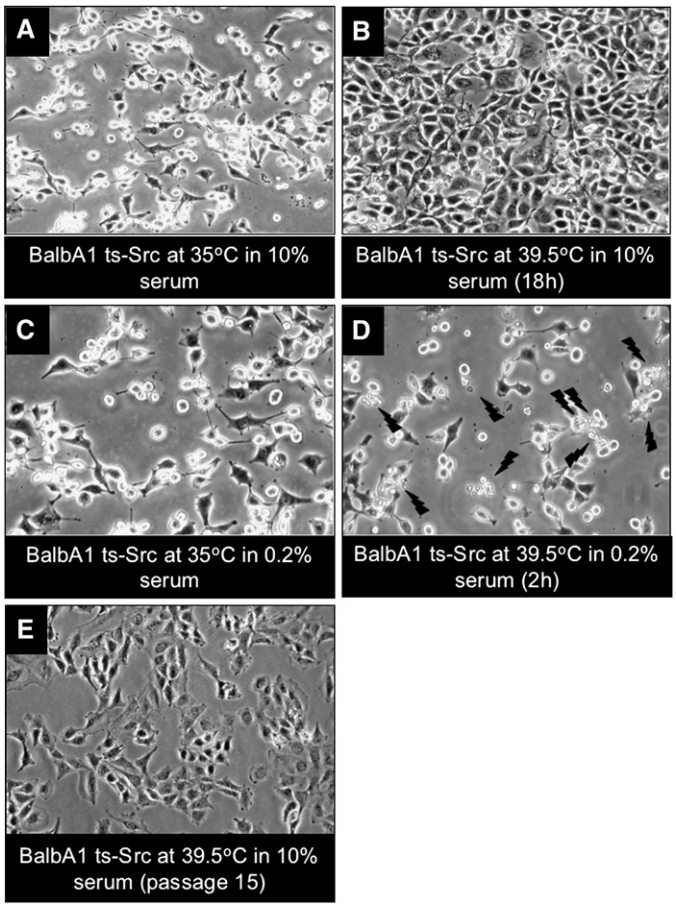


**Figure 3.** Morphological alterations induced by changes in serum and temperature in Balb-A1 ts-Src cells

**A:** Balb-A1 ts-Src cells growing in 10% serum-containing medium at 35°C display the typical transformed morphology of Src-transformed cells.
**B:** Overnight incubation at 39.5°C in the presence of 10% serum causes the cells to revert to a normal morphology.
**C:** Shown at a slightly higher magnification are Balb-A1 ts Src cells growing overnight in 0.2% serum-containing medium at 35°C.
**D:** When cells shown in **C** were shifted to 39.5°C (in 0.2% serum), cellular apoptosis was evident (indicated by jagged arrows) within 2 hr after the temperature shift.
**E:** Morphology of Balb-A1 ts-Src cells maintained continuously at 39.5°C in the presence of 10% serum, after 15 passages.

inactivation, levels of phospho-tyrosinated proteins rapidly begin to decline (Figure 4A), cleaved PARP begins to accumulate (Figure 4A), and levels of phospho-STAT3, -Akt, and -ERK1/2 are substantially diminished (Figure 4A). Moreover, levels of phospho-p38 begin to increase within 1 hr of Src inactivation and continue to increase until about 6 hr following temperature shift (Figure 4A).

To verify independently that the observed signaling changes following temperature shift truly reflect the consequences of Src inactivation, analogous studies were performed using a selective small molecule inhibitor of the Src kinase, SU-6656 (Blake et al., 2000). 3T3 mouse fibroblasts that had been transformed with a viral form of activated Src begin to exhibit apoptotic characteristics within 2 hr of treatment with SU-6656 and exhibit similar changes in the phosphorylation of STAT3, Akt, ERK1/2, and p38 proteins as seen in cells transformed by the temperature-sensitive Src mutant upon shift to the nonpermissive temperature (Figure 4B). Thus, the regulated phosphorylation of these proteins exhibits a kinetic profile upon Src inactivation that is analogous to that seen upon acute disruption of the BCR-ABL and activated EGFR kinases. Significantly, the signaling changes and apoptotic effects of Src inhibition with SU-6656 are only revealed in the absence of serum, consistent with a serum-provided survival signal that protects cells from the apoptotic output from oncogenic Src acutely following its inactivation (Figures S1 and S2 in the Supplemental Data available with this article online). Moreover, NIH3T3 cells expressing endogenous wild-type Src are unaffected by SU-6656 treatment even in the absence of serum, indicating that the observed apoptotic response is dependent on an output from oncogenic Src (Figure S3). Taken together, these findings suggest that a shared signaling cascade may contribute to ''addiction'' to Src, BCR-ABL, and EGFR kinases in cell culture models.

### Testing the model in a human tumor cell line

The three models of oncogene dependency described above are somewhat artificial in that they involve the introduction of a single oncogene into a cell type that may not correspond closely with the cell type that is malignantly transformed by the oncogene in the context of human tumorigenesis. Therefore, we performed a similar analysis of a human tumor-derived cell line that exhibits features associated with oncogene addiction. Specifically, we used the PC-9 human non-small cell lung cancer line, which harbors an activating mutation within the EGF receptor gene, and has been found to be exquisitely sensitive to the effects of gefitinib in a cell viability assay (Ono et al., 2004). Thus, 2 μM gefitinib kills the vast majority of these cells within 72 hr of treatment (Figure 5A), with levels of phospho-EGFR rapidly depleted within 4 hr of treatment (Figure 5B) and levels of cleaved PARP detectable within 8 hr of treatment (Figure 5B). We observed that levels of phospho-Akt and phospho-ERK1/2 in PC-9 cells are substantially diminished within 4 hr of gefitinib exposure (Figure 5B). Notably, phospho-Akt levels partially recover prior to apoptosis, consistent with the signal attenuation model described in the next section. Moreover, levels of phospho-p38 are observed to increase significantly beginning at 4 hr following gefitinib treatment, peaking by 8 hr, and persisting for 36 hr (Figure 5B). Hence, a profile of signal attenuation among these proteins is seen in gefitinib-treated human lung cancer cells and appears to be quite similar to the profile observed in each of the three models described above.

### Oncogene addiction may reflect the timing of signal attenuation

Since we observed that acute inactivation of Src, BCR-ABL, and EGFR oncogenes results in the rapid diminution of several cell survival effectors and the subsequent engagement of at least one proapoptotic effector, we wanted to examine a hypothesis that the apoptotic response to oncogene inactivation in these settings actually reflects a transient imbalance between prosurvival and proapoptotic signaling. To test this hypothesis, we utilized the temperature-sensitive Src-transformed cells, in which Src activity can be reversibly regulated. We reasoned that, if apoptosis in these cells following Src inactivation results from sustained proapoptotic signaling downstream of Src following rapid loss of prosurvival signals, it might be possible to ''protect''

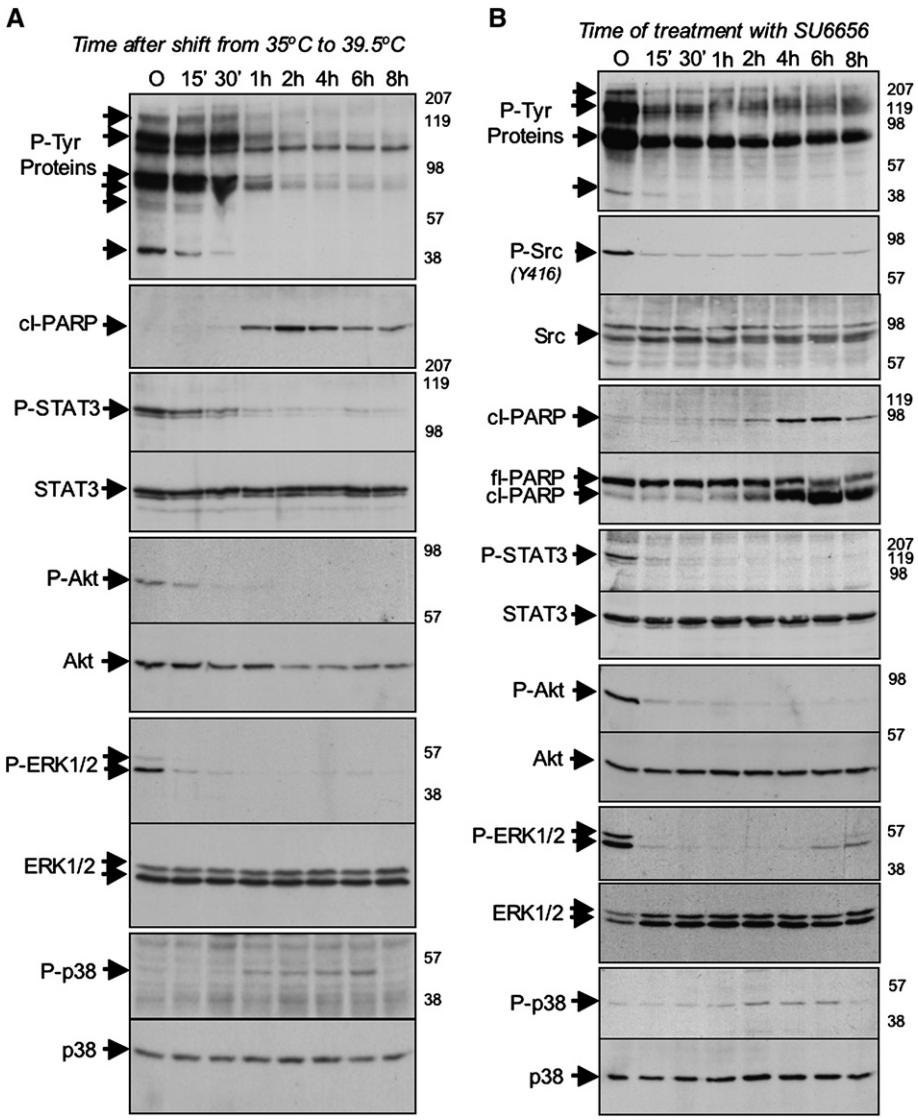


**Figure 4.** Modulation of signaling following acute Src inactivation in Balb-A1 ts-Src cells and ψ2 v-Src 3T3 cells

**A:** The ts-Src oncoprotein was inactivated in serum-starved Balb-A1 ts-Src cells by shifting cells to 39.5°C. At various times postinactivation of Src, cells were harvested and their proteins were analyzed by SDS-PAGE followed by western blotting using antibodies directed against phospho-tyrosine (P-Tyr proteins), cleaved PARP (cl-PARP), phospho-STAT3 (P-STAT3), STAT3, phospho-Akt (P-Akt), Akt, phospho-ERK1/2 (P-ERK1/2), ERK1/2, phospho-p38 (P-p38), and p38. Times postinactivation of Src (in minutes and hours) are indicated at the top of each lane, the relative migrations of the relevant proteins are indicated on the left-hand side of each autoradiogram, and to the right of each autoradiogram are indicated the relative migrations of molecular weight standards.

**B:** V-src oncoprotein was inactivated in serum-starved ψ2 v-Src 3T3 cells by the addition of 3 μM of SU-6656, a src-specific inhibitor. At various times postinactivation of Src, cells were harvested and their proteins were analyzed by SDS-PAGE followed by western blotting using antibodies directed against phospho-tyrosine (P-Tyr proteins), activated phospho-src (P-Src), total src, cleaved PARP (cl-PARP), full-length PARP (fl-PARP), phospho-STAT3 (P-STAT3), STAT3, phospho-Akt (P-Akt), Akt, phospho-ERK1/2 (P-RK1/2), ERK1/2, phospho-p38 (P-p38), and p38. Times postinactivation of Src (in minutes and hours) are indicated at the top of each lane, the relative migrations of the relevant proteins are indicated on the left-hand side of each autoradiogram, and to the right of each autoradiogram are indicated the relative migrations of molecular weight standards. In the top panel, arrows point to several unidentified proteins whose tyrosine phosphorylation appears to decrease upon v-src inactivation.

these cells from apoptosis following Src inactivation by culturing them for a period of time in serum (the survival factor) at 39.5°C prior to reducing serum to levels that would otherwise cause apoptosis in these cells.

First, we determined that inactivation of the PI-3 kinase/Akt pathway using the PI-3 kinase inhibitor LY294002 in cells maintained at 35°C in reduced serum (0.2%) causes a high percentage of cells to undergo apoptosis (Figure 6), indicating that serum is providing a PI-3 kinase-dependent cell survival signal in this context. Then, we observed that, when the Src-TS-transformed cells are initially propagated at 35°C (Src is activated) and then shifted to 39.5°C (Src is inactivated), they can be maintained in the presence of 10% serum indefinitely (Figure 3E). Moreover, the cells can then be transferred to low serum concentrations while remaining viable and without indications of apoptosis (data not shown). This finding clearly indicates that these Src-transformed cells are not absolutely dependent on Src activity for their survival and that they can be manipulated in such a way as to suppress the apoptotic response that can follow acute Src inactivation.

### Signal attenuation following oncogene activation may be temporally orchestrated via a phosphatase activity

The findings described above suggest that the kinetics of signal attenuation following acute inactivation of these various oncogenes contributes to the apoptotic response and that this could result from a transient imbalance in prosurvival and proapoptotic phosphorylation-mediated signaling. Moreover, the fact that each of these three oncogenic kinases (Src, BCR-ABL, and EGF receptor) has been reported to promote activation of the p38 MAP kinase (Bandyopadhyay et al., 2004; Harper et al., 2002; Turkson et al., 1999), and yet this kinase exhibits an apparent delayed activation upon oncogene inactivation, raises the possibility that relief from a phosphatase activity that suppresses levels of active phospho-p38 contributes to its delayed accumulation in these settings. In other words, we hypothesize that, while "steady-state" phospho-p38 levels appear to be relatively low in each of these cells prior to oncogene inactivation, this may reflect a dynamic balance between p38 phosphorylation and phosphatase-mediated dephosphorylation in which the phosphatase activity predominates.

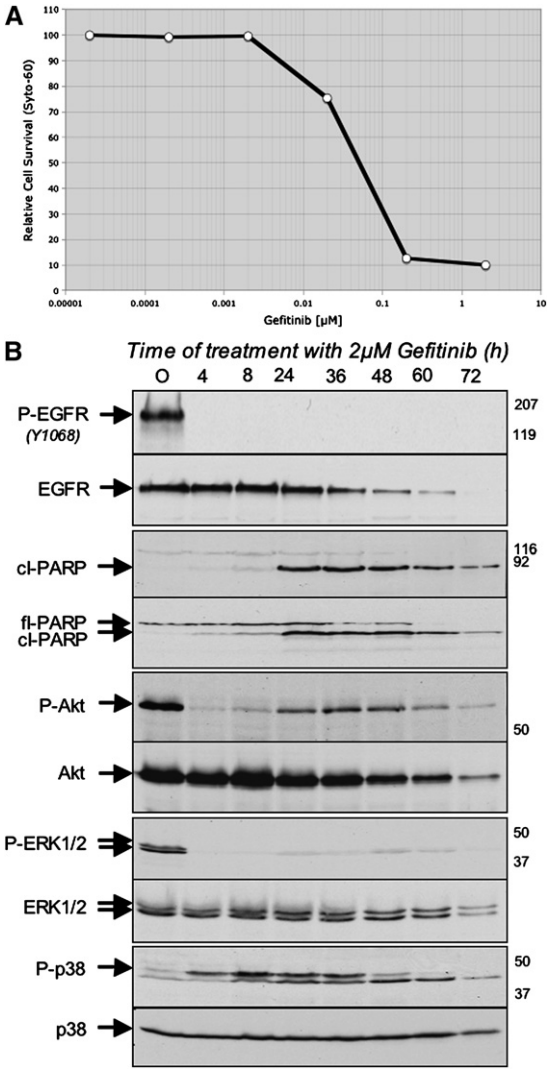


**Figure 5.** Modulation of signaling following acute EGFR inactivation in PC-9 cells

**A:** A dose-response curve for cell killing by gefitinib in subconfluent PC-9 cells following 72 hr of treatment with the inhibitor.

**B:** Activated EGFR in PC-9 cells was inactivated by the addition of 2 μM of gefitinib. At various times post-EGFR inactivation, cells were harvested and protein lysates were analyzed by SDS-PAGE followed by western blotting using antibodies directed against phospho-EGFR$^{Y1068}$ (P-EGFR), total EGFR, cleaved-PARP (cl-PARP), full-length PARP (fl-PARP), phospho-Akt (P-Akt), Akt, phospho-ERK1/2 (P-ERK1/2), ERK1/2, phospho-p38 (P-p38), and p38. Times postinactivation of EGFR (in hours) are indicated at the top of each lane, the relative migrations of the relevant proteins are indicated on the left-hand side of each autoradiogram, and to the right of each autoradiogram are indicated the relative migrations of molecular weight standards.

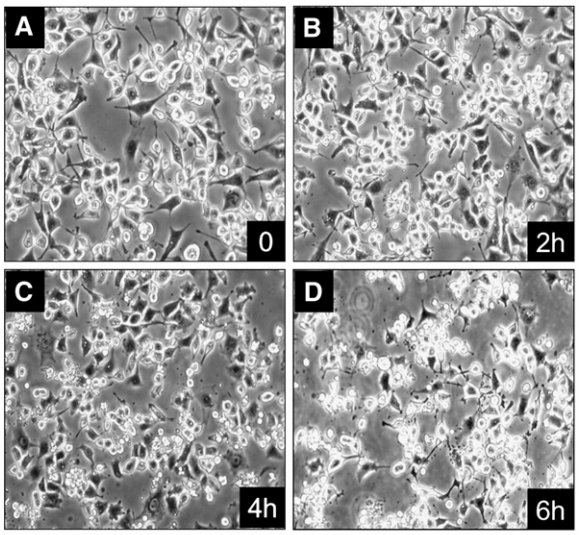


E

| TIME in LY294002 (50μM) | 0' | 15' | 30' | 60' | 2h | 4h | 6h | 24h |
|---|---|---|---|---|---|---|---|---|
| % survival (Crystal Violet) | 100 | 97 | 91 | 104 | 99 | **76** | **67** | **33** |

**Figure 6.** Effect of LY282004 on Balb-A1 ts-Src cells at 35°C in 0.2% serum

**A–D:** Serum-starved, Balb-A1 ts-Src cells were treated with 3 μM LY294002, and at various times posttreatment (0, 2, 4, and 6 hr) cell morphology was documented by photomicrography.

**E:** Cell survival was quantitated by crystal violet staining and tabulated.

To test this hypothesis, we treated the EGFR-transformed BAF3 cells with the phosphatase inhibitor okadaic acid (OA), which inhibits the PP2A phosphatase that has been previously shown to regulate phospho-p38 levels (Lee et al., 2003). As shown, OA treatment of these cells is sufficient to cause the accumulation of phospho-Akt, -ERK, and -p38 within 6 hr of treatment (Figure 7A; lanes 1–4), suggesting that the activation of these kinases is under negative regulatory control by an OA-sensitive phosphatase. Note that levels of phospho-EGFR eventually begin to decline, commensurate with the onset of apoptotic cell death in the population (Figure 7A; lanes 4 and 5). Then, we determined that the activation of these kinases by OA is largely suppressed by cotreatment with the EGFR inhibitor gefitinib (Figure 7B). Together, these observations suggest that a balance between EGFR kinase activity and an OA-sensitive phosphatase activity (possibly PP2A) contributes to the net phosphorylation status of several of the downstream mediators of EGFR-dependent prosurvival as well as proapoptotic signaling responses. These findings also implicate cellular phosphatases in orchestrating the timing of signal attenuation following acute inactivation of oncogenic kinases, such as the EGF receptor.

## Discussion

Oncogene addiction has now been well documented in several experimental cancer models and appears to play an important role in the clinical response to various targeted cancer therapies that have been recently developed. However, a clear molecular mechanism to explain the phenomenon of oncogene addiction has been somewhat elusive. Here, we have tested a specific hypothesis that oncogene addiction is associated with differences in the attenuation rates of multiple competing prosurvival and proapoptotic signals emanating from a single oncoprotein source. In three different cell culture models of oncogene dependency, we have observed a similar profile of rapid signal attenuation of several key survival effectors, and a temporally delayed accumulation of at least one proapoptotic effector, phospho-p38 MAP kinase. This signaling profile is also

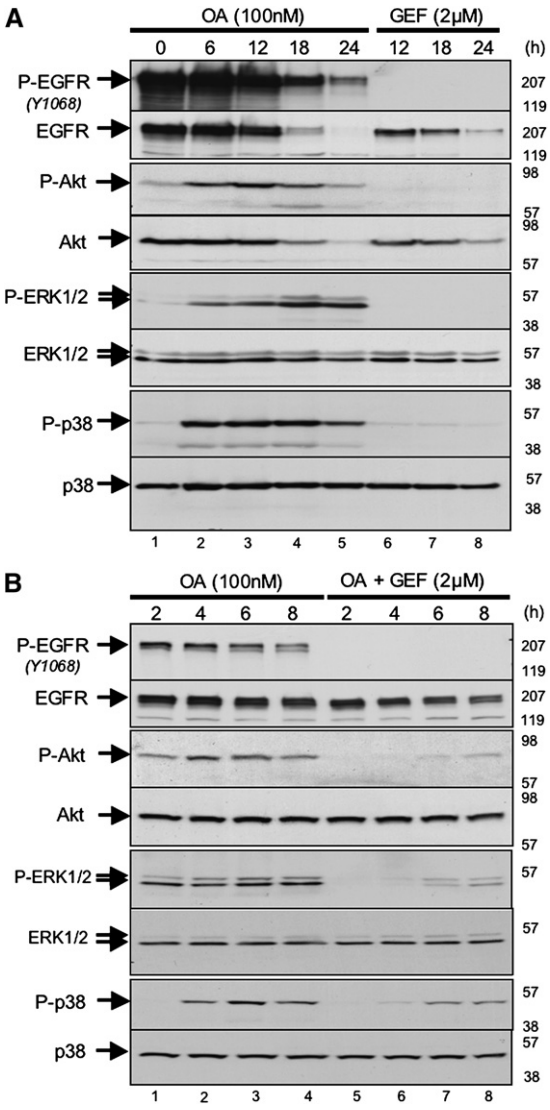


**Figure 7.** Effect of okadaic acid and gefitinib either singly or in combination on modulation of signaling in BaF3-EGFR(L858R) cells

BaF3-EGFR(L858R) cells were treated with either 100 nM okadaic acid (OA) alone (lanes 1–5 in **A**; lanes 1–4 in **B**), gefitinib (GEF) alone (lanes 6–8 in **A**), or 100 nM OA together with 2 μM gefitinib (lanes 5–8 in **B**). At various periods of time posttreatment (as indicated at the top of each lane), cells were harvested and their proteins were analyzed by SDS-PAGE followed by western blotting using antibodies directed against phospho-EGFR$^{Y1068}$ (P-EGFR), EGFR, phospho-Akt (P-Akt), Akt, phospho-ERK1/2 (P-ERK1/2), ERK1/2, phospho-p38 (P-p38), and p38. The relative migrations of the relevant proteins are indicated on the left-hand side of each autoradiogram, and to the right of each autoradiogram are indicated the relative migrations of molecular weight standards.

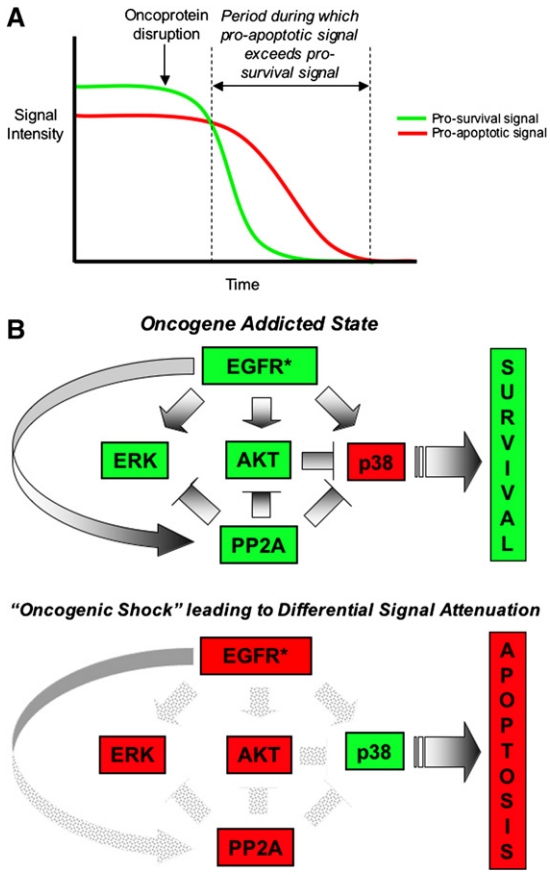


**Figure 8.** Proposed model of oncogene addiction

**A:** A graphical depiction of the proposed role of differential signal attenuation in creating a temporal window during which apoptotic signals persist in the absence of prosurvival signals following acute oncogene inactivation to promote cell death.

**B:** This model depicts the proposed role of differential signal attenuation in the cell death response to acute inactivation of oncogenic EGFR (EGFR*) upon which a tumor cell has become dependent. The upper panel illustrates the oncogene ''addicted'' state in which cells survive, and the lower panel illustrates the shift in the balance of prosurvival and proapoptotic signaling shortly following EGFR inactivation. Red, ''off''; green, ''on.''

observed in a human lung cancer cell line, PC-9, which harbors an activating EGF receptor mutation and is efficiently killed by a pharmacological concentration of gefitinib that exhibits efficacy in a subset of treated patients. These observations suggest that a common signaling cascade associated with coordinated timing of signal attenuation may underlie the apoptotic response to acute oncogene inactivation in the context of several different oncogenes and may also contribute to the clinical response to kinase inhibitors in a subset of cancer patients.

In this model of differential signal attenuation (Figure 8), we propose that, upon disruption of oncogenic activity, a temporary imbalance in proapoptotic and prosurvival signals results from the fact that at least some of the established survival factors, such as ERKs, Akt, and STAT3/5 undergo relatively rapid inactivation, whereas proapoptotic signals can persist long enough to drive an apoptotic outcome in the absence of counteracting survival signals. This model implies that a temporal window exists during which lingering ''unchecked'' proapoptotic signals emanating from an oncoprotein that has recently been inactivated cause the cell to pass a commitment point toward apoptosis. In fact, experimental studies have demonstrated that commitment to an apoptotic outcome can occur within only a few hours following the initiation of an apoptotic signal (Brunet et al., 1998). Our observation (especially in the PC-9 system) that phospho-AKT levels are rapidly inactivated for a brief period in lung cancer cells treated with the EGF receptor kinase inhibitor gefitinib, and then recover prior to apoptosis (Figure 5B), is consistent with a model wherein a transient loss of prosurvival signaling is

sufficient to shift the survival-death balance and to produce an apoptotic outcome. In addition, we have determined that transient transfection of cultured NIH3T3 cells with an activated Ras mutant that is specifically defective for interaction with the PI-3 kinase/Akt survival pathway causes apoptosis in a substantial fraction of transfected cells, whereas activated Ras that retains this interaction does not cause apoptosis (Figure S4).

While there are potentially multiple mechanisms that could contribute to a transient signaling imbalance following oncogene inactivation, the phosphatase inhibitor studies that we have described point to an important role for cellular phosphatases in determining the ''steady-state'' levels of phosphorylation of the various well-studied downstream effectors of many oncogenic kinases. These findings also implicate phosphatases in determining the temporal kinetics of effector activation and deactivation. While OA is an admittedly blunt tool for elucidating the precise mechanism by which phosphatases might contribute to differential signal attenuation, other reported studies similarly support a role for phosphatase activity in determining the temporal ordering of signal activation and deactivation. For example, previous studies of an apoptosis model in cultured PC12 neural cells that undergo apoptosis upon withdrawal of nerve growth factor revealed a similar temporally coordinated cascade of ERK1/2 inactivation followed by an accumulation of phospho-p38 prior to apoptosis (Xia et al., 1995). In addition, Akt has been reported to negatively regulate p38 activity, indirectly through the ASK1 and MKK3/6 kinases (Ichijo et al., 1997; Kim et al., 2001). Notably, protein phosphatase 5 (PP5), an OA-sensitive phosphatase, reportedly dephosphorylates ASK1 and inhibits ASK1 signaling (Morita et al., 2001), thereby providing another potential mechanism by which phosphatase activity could contribute to the timing of signal attenuation. These findings, together with our findings, suggest that a shared profile of orchestrated attenuation of prosurvival and proapoptotic signals may play an important role in a variety of apoptosis settings.

We recognize that we have only examined a relatively small subset of the numerous downstream effectors that have been previously implicated in the response to activating oncoproteins such as Src, EGF receptor, and BCR-ABL. Consequently, it is a near certainty that any differential signal attenuation mechanisms that may be operating in the models we have examined are more complex than the simple model we have described. Moreover, we note that multiple distinct mechanisms of oncogene addiction may be contributing to this phenomenon in the various contexts in which it has been observed. For example, the proliferative arrest and differentiation responses to oncogene inactivation that have been reported in some settings may involve distinct mechanisms, although it remains possible that an analogous signaling imbalance of a different nature could be contributing to those outcomes.

The proposed model of oncogene addiction differs somewhat from previous descriptions of the phenomenon in that it implies that the apoptotic outcome in response to oncogene inactivation is an active process that requires proapoptotic signals derived from the oncoprotein, as opposed to a passive process in which a cell that is dependent on an oncogene-derived survival signal defaults to an apoptotic death upon inactivation of that oncogene. It is well established that several oncoproteins, including Ras and Src, can produce proapoptotic outputs in some contexts (Arber, 1999; Webb et al., 2000). Moreover, most of the well-studied oncoproteins, such as EGF receptor, BCR-ABL, and Ras, promote the activation of numerous downstream effector pathways, and in each case, some of these have been linked to proapoptotic outcomes depending on the context. Several potential molecular mechanisms to account for a proapoptotic outcome have been reported. Thus, Ras can be proapoptotic via an interaction with the effector target Nore1 (Vos et al., 2003). Similarly, the EGF receptor can bind directly to the so-called ''death ligand'' FAS/CD95 (Reinehr et al., 2003). In addition, Src can induce apoptosis in B lymphocytes via engagement of the CD20 surface protein (Hofmeister et al., 2000). Thus, it is reasonable to expect that the state of a cell expressing an activated oncoprotein reflects the net balance of multiple diverse signaling pathways that have been engaged.

Accumulating evidence indicates that many tumor cells are poised on the edge of an apoptotic event and that tumor cells have an increased tendency to undergo apoptosis. In most tumor cells, the balance between prosurvival and proapoptotic signals clearly favors a survival outcome; however, it is easy to imagine that a temporary imbalance in those pathways in the initial hours following inactivation of the upstream source of those signals could shift cells toward an apoptotic event, particularly if the survival signals dissipate rapidly. Indeed, we have observed that treatment of PC-9 lung cancer cells for as little as 30 min (followed by drug washout) is sufficient to kill approximately half of the cells (Figure S5). Moreover, the differential signal attenuation model may also explain the emerging concept that tumor cells in which a kinase has undergone mutational activation or is overexpressed are especially sensitive to the killing effects of drugs that target those kinases. Specifically, the model suggests that increased kinase activity is associated with increased proapoptotic (as well as prosurvival) output, and that this excessive proapoptotic activity contributes to the cell death observed following acute inactivation of the oncogenic kinase. In support of such a conclusion, we have observed that cultured lung cancer cells that are killed by gefitinib treatment can be more efficiently killed in the presence of 10% serum, which contains EGF, the receptor ligand (Figure S6). This may reflect a role for EGF in driving higher levels of an apoptotic output from mutationally activated EGFR. In addition, this could explain why most normal cells, in which these same kinases are not signaling excessively, are typically not killed by treatment with a drug that targets the kinase. Thus, this differential signal attenuation model raises questions about the appropriateness of the term ''addiction'' in this setting, which seemingly implies a passive dependency on the oncogenic kinase. As an alternative, we have proposed the term ''oncogenic shock'' to describe the proposed signaling imbalance that can accompany acute oncogene inactivation, and which ascribes an active proapoptotic role to the oncogenic kinase in the consequent cell death response (Sharma et al., 2006). Notably, with such a mechanism, it may not be relevant whether the oncogenic lesion is an initiating event or a late event in tumorigenesis; however, its predominance in the tumor may be critical in determining whether targeting it produces a significant clinical response.

The studies we have performed may also have clinical implications regarding the use of cancer therapies that target oncogenic kinases. For example, coadministration of a drug that promotes cell cycle arrest might suppress apoptosis that would normally be triggered by acute inactivation of an oncogenic kinase, a mechanism that has potentially contributed to the

disappointing results observed thus far when EGFR kinase inhibitors are administered together with conventional chemotherapy drugs. These findings also raise the possibility that drugs directed against downstream signaling proteins that shift the balance of kinase-mediated proapoptotic and prosurvival signals may also have therapeutic value. Differential signal attenuation may also contribute to the acquisition of drug resistance that frequently develops in patients during treatment with selective kinase inhibitors if genetic or epigenetic changes allow cells to survive during a temporal window between the dissipation of prosurvival and proapoptotic signals. These findings also raise the possibility that "on-off cycles," as opposed to continuous treatment, with targeted kinase inhibitors may be more beneficial to patients by allowing for more "windows of opportunity" for the inhibitors to produce a transient signaling imbalance that leads to apoptotic cell death. Thus, in contrast to traditional chemotherapeutic agents that appear to trigger a DNA damage response, the emergence of small molecules that target specific components of signaling pathways may involve distinct mechanisms of cancer cell death. Further insights into these mechanisms may allow optimal clinical application of these new molecularly targeted agents.

## Experimental procedures

### Cell lines

TonB210.1 cells expressing the tetracycline-inducible Bcr-Abl oncogene were kindly provided by George Q. Daley (Children's Hospital, Boston) and were maintained as described previously (Klucher et al., 1998). BaF3-EGFR expressing the gefitinib-sensitizing L858R mutant EGFR was maintained as described previously (Jiang et al., 2005). PC-9 cells expressing the gefitinib-sensitizing deletion mutation (ΔE746-A750) were kindly provided by Dr. Kazuto Nishio (National Cancer Center Hospital, Tokyo) and were maintained as described previously (Koizumi et al., 2005). Balb A1-ts src cells expressing the temperature-sensitive v-src oncogene and Ψ2 v-src 3T3 cells expressing the retroviral v-src oncogene were propagated in DMEM containing 10% fetal bovine serum (FBS) and penicillin and streptomycin (100 U/ml and 100 mg/ml, respectively). NIH 3T3 mouse fibroblasts were maintained in DMEM supplemented with 10% calf serum and penicillin and streptomycin (100 U/ml and 100 g/ml, respectively).

### Antibodies

HRP-conjugated anti-phosphotyrosine antibody and rabbit polyclonal antibody against phospho-Akt (Ser473) were purchased from Biosource. The rabbit polyclonal antibody directed against EGFR was from Santa Cruz Biotechnology. Mouse monoclonal antibodies against phospho-EGFR (Tyr1068), phospho-STAT5 (Tyr694), and cleaved PARP as well as rabbit polyclonal antibodies against Bcr, phospho-p44/42 ERK kinase (Thr202/Tyr204), phospho-Akt (Ser473), phospho-Src (Tyr416), phospho-STAT3 (Tyr705), full-length PARP, and phospho-p38 (Thr180/Tyr182), and antibodies directed against their nonphosphorylated counterparts, were purchased from Cell Signaling Technology. Anti-BrdU antibody was from Becton Dickinson. Secondary antibodies included HRP-conjugated anti-mouse and anti-rabbit antibodies and were purchased from Cell Signaling Technology. The FITC-conjugated anti-mouse antibody was from Vector Laboratories.

### Inhibitors

Gefitinib was kindly provided be Astra-Zeneca Pharmaceuticals (Macclesfield, UK) and was resuspended in DMSO at a stock concentration of 2 mM. OA, LY282004, and the Src-specific inhibitor SU6656 were purchased from Calbiochem and resuspended in DMSO at a stock concentration of 0.1, 50, and 5 mM, respectively. All inhibitors were stored in small aliquots at −20°C.

### Induction of apoptosis by oncogene inactivation

Cells were plated in their respective maintenance media and used for experimentation when they had reached a confluence of 70%. Apoptosis was induced in each system as described below. At various times after induction of apoptosis, the cells were harvested, and the activation state of the relevant signal transducers was assessed by SDS-PAGE followed by western blotting.

### Bcr-Abl

The Bcr-Abl protein was induced in TonB-210.1 cells by incubating them for 18 hr with 1 μg/ml of doxycycline in their growth medium (RPMI-1640 containing sodium pyruvate, penicillin-streptomycin, and 10% FBS). Inactivation of Bcr-Abl was accomplished by the removal of doxycycline from the growth medium. To this end, cells were collected by centrifugation, washed three times in media without doxycycline, and resuspended in media without doxycycline, and at various times (0, 1, 2, 4, 8, 24, 48, and 72 hr) cells were harvested for analysis.

### Src

Exponentially growing Balb A1-ts src cells growing at 35°C in DMEM containing 10% FBS were washed once with DMEM containing 0.2% FBS and then placed in DMEM containing 0.2% FBS at 35°C for a period of 18 hr. V-src was inactivated by replacing the medium on the cells with DMEM containing 0.2% FBS that had been prewarmed to 39.5°C. At various times postinactivation of src (0, 15 min, 30 min, 1 hr, 2 hr, 4 hr, 6 hr, and 8 hr), cells were harvested for analysis.

Exponentially growing Ψ2 v-src 3T3 cells were washed once with serum-free DMEM and then placed in serum-free DMEM for a period of 18 hr. Subsequently, they were treated with 3 μM SU6656 (in DMSO) that was added directly to the serum-free growth medium. The untreated controls received an equivalent volume of DMSO. Following treatment with SU6656, cells were harvested at 0, 15 min, 30 min, 1 hr, 2 hr, 4 hr, 6 hr, and 8 hr.

### EGFR

Exponentially growing BaF3-EGFR(L858R) and PC-9 cells were treated with 2 μM gefitinib (in DMSO) that was added directly to the growth medium (RPMI-1640 containing sodium pyruvate, penicillin-streptomycin, and 10% FBS). The untreated controls received an equivalent volume of DMSO. Following treatment with gefitinib, cells were harvested at 0, 4, 8, 24, 36, 48, 60, and 72 hr. In experiments using BaF3-EGFR(L858R), which involved the use of OA shown in Figure 8, OA was used at a final concentration of 100 nM and was added either by itself or together with gefitinib for the appropriate amounts of time as indicated in the figure.

### Transfection and apoptosis assays

Transfection of NIH 3T3 mouse fibroblasts was performed with an electroporator using reagents and protocols provided by the manufacturer (Amaxa). Cells were transfected with 1 μg of vector, H-Ras$^{V12}$, or H-Ras$^{V12}$T35S (White et al., 1995) together with a GFP plasmid provided by Amaxa (to monitor transfection efficiency). Six to eight hours following transfection, cells were washed and transferred to DMEM containing 0.1% FBS. At this time, the transfection efficiency was also assayed by fluorescence microscopy of GFP signal and determined to be approximately 80%–90%. Cell number and apoptosis were assayed 40 hr later. The number of cells that adhered to the dish is presented as a percentage of cells relative to vector-transfected controls (Figure S4A). Apoptotic cells were quantitated using fluorescence-activated cell sorting (FACS) according to the manufacturer's protocol (Becton Dickinson). Cells were incubated with cell-labeling reagent BrdU (Amersham-Pharmacia) at 37°C for 30 min. Subsequently, all cells (adherent and floating) were collected, washed with PBS, and fixed in 80% ethanol. DNA was denatured for 30 min with 2 M HCl/0.5% Triton X-100 and neutralized with 0.1 M $NaB_4O_7 \bullet 10\ H_2O$ (pH 8.5), before incubation with anti-BrdU antibody (1:500) and a FITC-conjugated goat anti-mouse secondary antibody (1:50). Cells were stained with 5 μg/ml propidium iodide (Sigma) and treated with RNase A (Sigma) prior to two-dimensional FACS analysis using CELLQUEST software (Becton Dickinson). The number of gated cells in the sub-G1 population is presented as the ratio of apoptotic cells to vector-transfected controls (Figure S4B).

### Cell harvesting and protein analysis

At each time point, cells were placed on ice, scraped in their own media, and collected by low-speed refrigerated centrifugation. Cell pellets were then

washed once in ice-cold PBS and stored at −80°C until ready for analysis by SDS-PAGE and immunoblotting using standard procedures.

**Supplemental data**

The Supplemental Data include six supplemental figures and can be found with this article online at http://www.cancercell.org/cgi/content/full/10/5/425/DC1/.

**Acknowledgments**

We are grateful to members of the Settleman and Haber laboratories and Michael Fischbach for helpful discussions. We thank Matthew Meyerson for providing the BAF3-EGFR cells, George Daley for the TonB210.1 cells, and Joan Brugge for the TS-Src plasmid. This work was supported by NIH RO1 CA115830, a V Foundation Award, and a Saltonstall Scholar Award to J.S.

Received: April 10, 2006
Revised: July 10, 2006
Accepted: September 8, 2006
Published: November 13, 2006

**References**

Aoki, K., Yoshida, T., Matsumoto, N., Ide, H., Sugimura, T., and Terada, M. (1997). Suppression of Ki-ras p21 levels leading to growth inhibition of pancreatic cancer cell lines with Ki-ras mutation but not those without Ki-ras mutation. Mol. Carcinog. *20*, 251–258.

Arber, N. (1999). Janus faces of ras: Anti or pro-apoptotic? Apoptosis *4*, 383–388.

Bandyopadhyay, G., Biswas, T., Roy, K.C., Mandal, S., Mandal, C., Pal, B.C., Bhattacharya, S., Rakshit, S., Bhattacharya, D.K., Chaudhuri, U., et al. (2004). Chlorogenic acid inhibits Bcr-Abl tyrosine kinase and triggers p38 mitogen-activated protein kinase-dependent apoptosis in chronic myelogenous leukemic cells. Blood *104*, 2514–2522.

Blake, R.A., Broome, M.A., Liu, X., Wu, J., Gishizky, M., Sun, L., and Courtneidge, S.A. (2000). SU6656, a selective src family kinase inhibitor, used to probe growth factor signaling. Mol. Cell. Biol. *20*, 9018–9027.

Brunet, C.L., Gunby, R.H., Benson, R.S., Hickman, J.A., Watson, A.J., and Brady, G. (1998). Commitment to cell death measured by loss of clonogenicity is separable from the appearance of apoptotic markers. Cell Death Differ. *5*, 107–115.

Chin, L., Tam, A., Pomerantz, J., Wong, M., Holash, J., Bardeesy, N., Shen, Q., O'Hagan, R., Pantginis, J., Zhou, H., et al. (1999). Essential role for oncogenic Ras in tumour maintenance. Nature *400*, 468–472.

Druker, B.J., Tamura, S., Buchdunger, E., Ohno, S., Segal, G.M., Fanning, S., Zimmermann, J., and Lydon, N.B. (1996). Effects of a selective inhibitor of the Abl tyrosine kinase on the growth of Bcr-Abl positive cells. Nat. Med. *2*, 561–566.

Felsher, D.W., and Bishop, J.M. (1999). Reversible tumorigenesis by MYC in hematopoietic lineages. Mol. Cell *4*, 199–207.

Gambacorti-Passerini, C., le Coutre, P., Mologni, L., Fanelli, M., Bertazzoli, C., Marchesi, E., Di Nicola, M., Biondi, A., Corneo, G.M., Belotti, D., et al. (1997). Inhibition of the ABL kinase activity blocks the proliferation of BCR/ABL+ leukemic cells and induces apoptosis. Blood Cells Mol. Dis. *23*, 380–394.

Harper, M.E., Goddard, L., Glynne-Jones, E., Assender, J., Dutkowski, C.M., Barrow, D., Dewhurst, O.L., Wakeling, A.E., and Nicholson, R.I. (2002). Multiple responses to EGF receptor activation and their abrogation by a specific EGF receptor tyrosine kinase inhibitor. Prostate *52*, 59–68.

Hofmeister, J.K., Cooney, D., and Coggeshall, K.M. (2000). Clustered CD20 induced apoptosis: Src-family kinase, the proximal regulator of tyrosine phosphorylation, calcium influx, and caspase 3-dependent apoptosis. Blood Cells Mol. Dis. *26*, 133–143.

Huettner, C.S., Zhang, P., Van Etten, R.A., and Tenen, D.G. (2000). Reversibility of acute B-cell leukaemia induced by BCR-ABL1. Nat. Genet. *24*, 57–60.

Ichijo, H., Nishida, E., Irie, K., ten Dijke, P., Saitoh, M., Moriguchi, T., Takagi, M., Matsumoto, K., Miyazono, K., and Gotoh, Y. (1997). Induction of apoptosis by ASK1, a mammalian MAPKKK that activates SAPK/JNK and p38 signaling pathways. Science *275*, 90–94.

Jiang, J., Greulich, H., Janne, P.A., Sellers, W.R., Meyerson, M., and Griffin, J.D. (2005). Epidermal growth factor-independent transformation of Ba/F3 cells with cancer-derived epidermal growth factor receptor mutants induces gefitinib-sensitive cell cycle progression. Cancer Res. *65*, 8968–8974.

Johnson, D., Agochiya, M., Samejima, K., Earnshaw, W., Frame, M., and Wyke, J. (2000). Regulation of both apoptosis and cell survival by the v-Src oncoprotein. Cell Death Differ. *7*, 685–696.

Kim, A.H., Khursigara, G., Sun, X., Franke, T.F., and Chao, M.V. (2001). Akt phosphorylates and negatively regulates apoptosis signal-regulating kinase 1. Mol. Cell. Biol. *21*, 893–901.

Klucher, K.M., Lopez, D.V., and Daley, G.Q. (1998). Secondary mutation maintains the transformed state in BaF3 cells with inducible BCR/ABL expression. Blood *91*, 3927–3934.

Koizumi, F., Shimoyama, T., Taguchi, F., Saijo, N., and Nishio, K. (2005). Establishment of a human non-small cell lung cancer cell line resistant to gefitinib. Int. J. Cancer *116*, 36–44.

Lee, T., Kim, S.J., and Sumpio, B.E. (2003). Role of PP2A in the regulation of p38 MAPK activation in bovine aortic endothelial cells exposed to cyclic strain. J. Cell. Physiol. *194*, 349–355.

Lynch, T.J., Bell, D.W., Sordella, R., Gurubhagavatula, S., Okimoto, R.A., Brannigan, B.W., Harris, P.L., Haserlat, S.M., Supko, J.G., Haluska, F.G., et al. (2004). Activating mutations in the epidermal growth factor receptor underlying responsiveness of non-small-cell lung cancer to gefitinib. N. Engl. J. Med. *350*, 2129–2139.

Maroney, A.C., Qureshi, S.A., Foster, D.A., and Brugge, J.S. (1992). Cloning and characterization of a thermolabile v-src gene for use in reversible transformation of mammalian cells. Oncogene *7*, 1207–1214.

Morita, K., Saitoh, M., Tobiume, K., Matsuura, H., Enomoto, S., Nishitoh, H., and Ichijo, H. (2001). Negative feedback regulation of ASK1 by protein phosphatase 5 (PP5) in response to oxidative stress. EMBO J. *20*, 6028–6036.

Mukohara, T., Engelman, J.A., Hanna, N.H., Yeap, B.Y., Kobayashi, S., Lindeman, N., Halmos, B., Pearlberg, J., Tsuchihashi, Z., Cantley, L.C., et al. (2005). Differential effects of gefitinib and cetuximab on non-small-cell lung cancers bearing epidermal growth factor receptor mutations. J. Natl. Cancer Inst. *97*, 1185–1194.

O'Dwyer, M.E., Mauro, M.J., and Druker, B.J. (2003). STI571 as a targeted therapy for CML. Cancer Invest. *21*, 429–438.

Ono, M., Hirata, A., Kometani, T., Miyagawa, M., Ueda, S., Kinoshita, H., Fujii, T., and Kuwano, M. (2004). Sensitivity to gefitinib (Iressa, ZD1839) in non-small cell lung cancer cell lines correlates with dependence on the epidermal growth factor (EGF) receptor/extracellular signal-regulated kinase 1/2 and EGF receptor/Akt pathway for proliferation. Mol. Cancer Ther. *3*, 465–472.

Paez, J.G., Janne, P.A., Lee, J.C., Tracy, S., Greulich, H., Gabriel, S., Herman, P., Kaye, F.J., Lindeman, N., Boggon, T.J., et al. (2004). EGFR mutations in lung cancer: Correlation with clinical response to gefitinib therapy. Science *304*, 1497–1500.

Pao, W., Miller, V., Zakowski, M., Doherty, J., Politi, K., Sarkaria, I., Singh, B., Heelan, R., Rusch, V., Fulton, L., et al. (2004). EGF receptor gene mutations are common in lung cancers from "never smokers" and are associated with sensitivity of tumors to gefitinib and erlotinib. Proc. Natl. Acad. Sci. USA *101*, 13306–13311.

Reinehr, R., Schliess, F., and Haussinger, D. (2003). Hyperosmolarity and CD95L trigger CD95/EGF receptor association and tyrosine phosphorylation of CD95 as prerequisites for CD95 membrane trafficking and DISC formation. FASEB J. *17*, 731–733.

Sharma, S.V., Fischbach, M.A., Haber, D.A., and Settleman, J. (2006). "Oncogenic shock": Explaining oncogene addiction through differential signal attenuation. Clin. Cancer Res. *12*, 4392s–4395s.

Steelman, L.S., Pohnert, S.C., Shelton, J.G., Franklin, R.A., Bertrand, F.E., and McCubrey, J.A. (2004). JAK/STAT, Raf/MEK/ERK, PI3K/Akt and BCR-ABL in cell cycle progression and leukemogenesis. Leukemia *18*, 189–218.

Turkson, J., Bowman, T., Adnane, J., Zhang, Y., Djeu, J.Y., Sekharam, M., Frank, D.A., Holzman, L.B., Wu, J., Sebti, S., and Jove, R. (1999). Requirement for Ras/Rac1-mediated p38 and c-Jun N-terminal kinase signaling in Stat3 transcriptional activity induced by the Src oncoprotein. Mol. Cell. Biol. *19*, 7519–7528.

Vos, M.D., Martinez, A., Ellis, C.A., Vallecorsa, T., and Clark, G.J. (2003). The pro-apoptotic Ras effector Nore1 may serve as a Ras-regulated tumor suppressor in the lung. J. Biol. Chem. *278*, 21938–21943.

Webb, B.L., Jimenez, E., and Martin, G.S. (2000). v-Src generates a p53-independent apoptotic signal. Mol. Cell. Biol. *20*, 9271–9280.

Weinstein, I.B. (2000). Disorders in cell circuitry during multistage carcinogenesis: The role of homeostasis. Carcinogenesis *21*, 857–864.

Weinstein, I.B. (2002). Cancer. Addiction to oncogenes—The Achilles heal of cancer. Science *297*, 63–64.

Weinstein, I.B., Begemann, M., Zhou, P., Han, E.K., Sgambato, A., Doki, Y., Arber, N., Ciaparrone, M., and Yamamoto, H. (1997). Disorders in cell circuitry associated with multistage carcinogenesis: Exploitable targets for cancer prevention and therapy. Clin. Cancer Res. *3*, 2696–2702.

White, M.A., Nicolette, C., Minden, A., Polverino, A., Van Aelst, L., Karin, M., and Wigler, M.H. (1995). Multiple Ras functions can contribute to mammalian cell transformation. Cell *80*, 533–541.

Xia, Z., Dickens, M., Raingeaud, J., Davis, R.J., and Greenberg, M.E. (1995). Opposing effects of ERK and JNK-p38 MAP kinases on apoptosis. Science *270*, 1326–1331.